JOURNAL OF MATERIALS SCIENCE **37** (2002) 3631 – 3639

Processing sodium tellurite melts in low gravity drop shaft

Part I *Melt evaporation and formation of solid particles from vapor*

DONGMEI ZHU
Ceramic Engineering Department and Graduate Center for Materials Research, University of Missouri-Rolla, Rolla, MO 65409, USA; State Key Laboratory of Solidification Processing, Northwestern Polytechnic University, Xi'an, Shaanxi 710072, People's Republic of China
E-mail: dzhu@umr.edu

C. S. RAY
Ceramic Engineering Department and Graduate Center for Materials Research, University of Missouri-Rolla, Rolla, MO 65409, USA

M. MAKIHARA
Department of Optical Materials, Osaka National Research Institute, 1-8-31 Midorigaoka, Ikeda, Osaka 563-8577, Japan

WANCHENG ZHOU
State Key Laboratory of Solidification Processing, Northwestern Polytechnic University, Xi'an, Shaanxi 710072, People's Republic of China

D. E. DAY
Ceramic Engineering Department and Graduate Center for Materials Research, University of Missouri-Rolla, Rolla, MO 65409, USA

Glasses of $Na_2O \cdot 8TeO_2$ and $Na_2O \cdot 4TeO_2$ compositions adhered to a small platinum heating coil (2 to 3 mm ID, 5 to 6 mm long) were melted and evaporated in low gravity using the drop shaft at the Japan Microgravity Center (JAMIC). The gravity level attained during the 10 s free fall was in the order of 10^{-3} g. The species evaporated from the melt in low gravity generally formed a spherical smoke cloud surrounding the melt, whose size depended on the melt temperature and also on the time the melt evaporated in low gravity. The shape of the cloud was found to depend on several other factors, namely, the uniformity of heating, amount of melt, and the presence of gas bubbles in the melt. The evaporating species formed nearly perfect spheres of pure TeO_2 whose diameter ranged from 0.05 to 20 μm. The size of TeO_2 microspheres increased with increasing melt temperature and time in low gravity, and was 5 to 10 times larger than that of similar particles prepared at 1-g.

1. Introduction

Microgravity is a special and unique experimental environment for materials processing. The absence or near absence of gravity-driven convection in low gravity decreases the rates of sedimentation and mass transport, hydrostatic pressure and buoyancy-driven flow. Many weak, physical forces such as surface tension and diffusion, which generally remain masked by gravity-driven convection at 1-g become prominent and measurable in low gravity, thereby, providing the opportunity to identify their role in materials processing. This unique environment can be used to prepare new and ultra-pure materials, or composite materials containing components whose liquids undergo spontaneous phase separation.

Since buoyancy-driven flows are believed to promote rapid mixing in liquids/melts, it is generally thought that the chemical homogeneity of a glass prepared by quenching a melt in low gravity would be no better than that of a similar glass prepared at normal gravity. However, there are reports [1–7] which indicate that glasses prepared in low gravity are more chemically homogeneous and also more resistant to crystallization than identical glasses prepared at 1-g. At the same time, the glass has smaller and fewer micro-heterogeneous regions and is more resistant to crystallization. It appears that the solidification mechanism of glasses in low gravity may be different from that on earth.

Studies on the growth of solid particles from vapor in low gravity provide new and important information

on the kinetics of nucleation and growth for vapor-liquid-solid phase transformation [8]. Because of the drastic reduction of the hydrostatic pressure in microgravity, liquid droplets should not deform under their own weight and particles of more uniform size and spherical shape will be obtained in low gravity. Glass microspheres of uniform shape and size have many potential applications, such as radiation delivery vehicles in medicine [9, 10], microresonators in microspherical lasers [11] and inertial confinement fusion (ICF) targets [12].

The present work is primarily a continuation of our work previously conducted in the drop shaft at Japan Microgravity center (JAMIC) for the purpose of understanding more about the phenomena of melt evaporation, formation of solid particles from vapor, and glass formation/crystallization of sodium tellurite melts in low gravity. The main variables in the experiments described herein were the melt temperature, and the substrate materials on which the melts splattered and solidified during the high-g deceleration of the drop capsule. The results from these low gravity experiments are compared with those from experiments conducted at 1-g using the same temperature-time profile for melting and the same substrate materials used in low gravity experiments. In the present paper, the results for melt evaporation and formation of solid particles from a vapor in low gravity are described and discussed. The glass formation/crystallization behavior of these melts is discussed in a second paper.

2. Experiments

2.1. Drop apparatus

The apparatus used for the drop experiments is shown schematically in Fig. 1. It consists of a glass box (A), a platinum heating coil (B) holding the glass sample and a Platinum-13% Rhodium thermocouple (C). The glass box (A) of approximate dimension, 5.0 cm × 5.0 cm × 7.6 cm, was prepared using glass microscope slides except for the bottom plate which was made of different materials, such as glass, alumina, copper, gold and platinum. The heating coil, ∼5 mm long and 3 mm internal diameter, was prepared using 0.3 mm diameter platinum wire (∼15 turns). The two ends of the heating coil were attached to ∼2 mm diameter copper wire leads (D), held in a two-hole refractory tube (E), and connected to a power supply. The purpose of using low resistance (thick) copper leads was to minimize the heat loss and to obtain a high temperature (at the coil) with a relatively low power input.

The refractory tube (F) holding the thermocouple was fastened to the refractory tube (E) holding the heating coil after positioning the thermocouple tip at the approximate center of the coil. This arrangement ensures a fixed position of the thermocouple tip during the entire experiment. An appropriate amount of glass (typically from 60 to 280 mg) was fused to the coil by passing a small current through the coil, which was just sufficient to melt the glass. The amount of glass was adjusted so that the melt was held (due to surface tension) by the coil at 1-g. The power to the coil was then turned off (the melt solidified to glass) and the thermocouple tip was securely imbedded inside the glass. The position of the thermocouple did not change during normal handling.

The platinum coil assembly holding the melt and thermocouple was placed at the approximate center of the glass box (A), the distance between the coil and the bottom plate being about 4 cm. The box was attached to a frame (G) where a video and a 35 mm camera were also attached to record the entire experiment. The two cameras were placed perpendicular to each other, the video camera being perpendicular to the axis of the heating coil.

The drop capsule consists of three parts. The middle part of the capsule contains the experimental package. A schematic of the drop capsule and the drop shaft at JAMIC are shown in Fig. 2. The experiments were conducted in air at normal atmospheric pressure.

2.2. Glass preparation

The $Na_2O \cdot 8TeO_2 (NT_8)$ and $Na_2O \cdot 4TeO_2$ (NT_4) glasses used in the present experiments were prepared by melting mixtures of Na_2CO_3 (purity 99.95%) and TeO_2 (purity 99.99%) in appropriate amounts in a platinum crucible in air between 750 and 800°C for 0.5 to 1.0 h and quenching the melts between two steel plates. Transparent glass was obtained for both compositions, NT_8 and NT_4, and no crystalline or unmelted particles were detected by X-ray diffraction analysis (XRD).

2.3. Heating schedule for drop experiments

A typical heating schedule programmed for the drop experiments, which is shown schematically in Fig. 3,

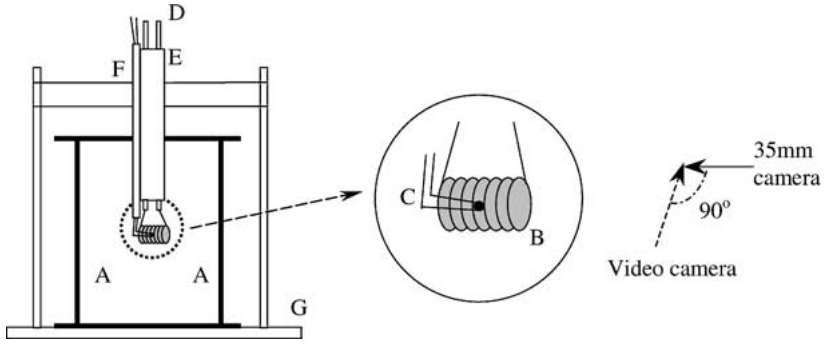

Figure 1 Schematic of the apparatus used for low-gravity experiments in the JAMIC drop shaft. A: Glass box, B: Platinum heating coil holding the glass sample, C: Pt-Pt/13%Rh thermocouple, D: Copper wire leads, E: Refractory tube holding heating coil, F: Refractory tube holding thermocouple, G: Main frame.

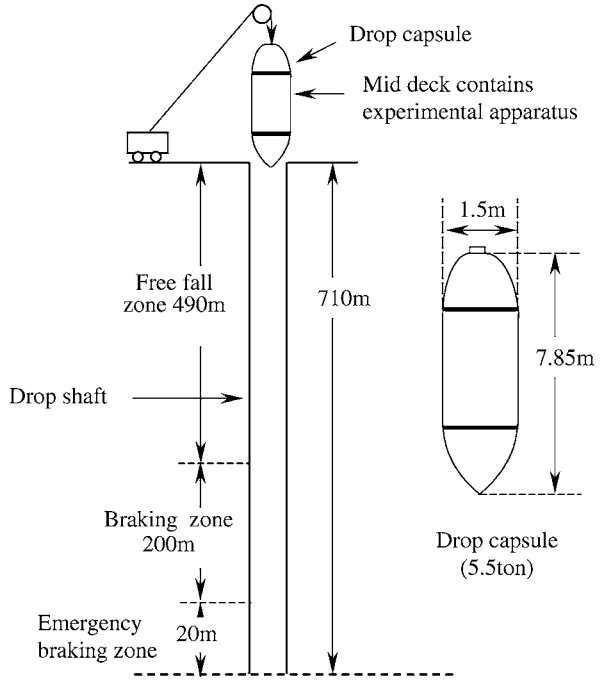

Figure 2 Schematic of drop capsule and drop shaft at Japan Microgravity Center (JAMIC).

generally consists of four stages. In the first stage, which starts about 2.5 min before the capsule is released, the voltage to the heating coil is gradually increased over 30 s, so that the glass in the coil attains a temperature of ~200°C (first preheating stage). After a pause of 30 s, the voltage is again gradually increased for 30 s to a temperature between 400 and 425°C, which is about 75 to 50°C lower than the melting temperature of the glass (second preheating stage). The third stage begins just 1 s before capsule release, when the voltage to the coil is rapidly increased to a pre-set maximum, causing the glass to melt and evaporate. The power to the coil is turned off (fourth stage) ~7 s after capsule release, i.e., ~3 s before the capsule starts decelerating (total low gravity time ~10 s). The voltage takes ~1 s to reach zero. All four experimental stages are programmed before the drop apparatus (Fig. 1) is installed in the capsule and executed remotely from the control room.

3. Result and discussion

3.1. Melting and evaporation of samples

Fig. 4 shows the typical gravity level (Z-direction, vertical to the axis of the heating coil) during free fall of the capsule at JAMIC. The gravity value for all the experiments was highly reproducible and is the same as that shown in Fig. 4. The value of gravity was

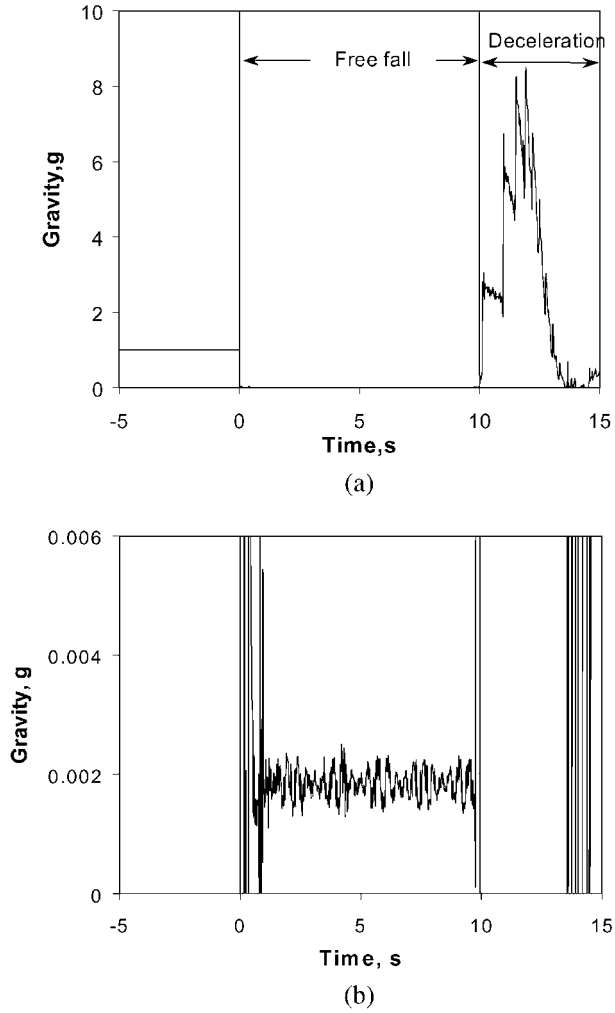

Figure 4 Typical gravity level (Z-direction, vertical to the axis of the heating coil) during free fall and braking of the capsule at JAMIC, (a) condensed scale, (b) extended scale in units of normal gravity.

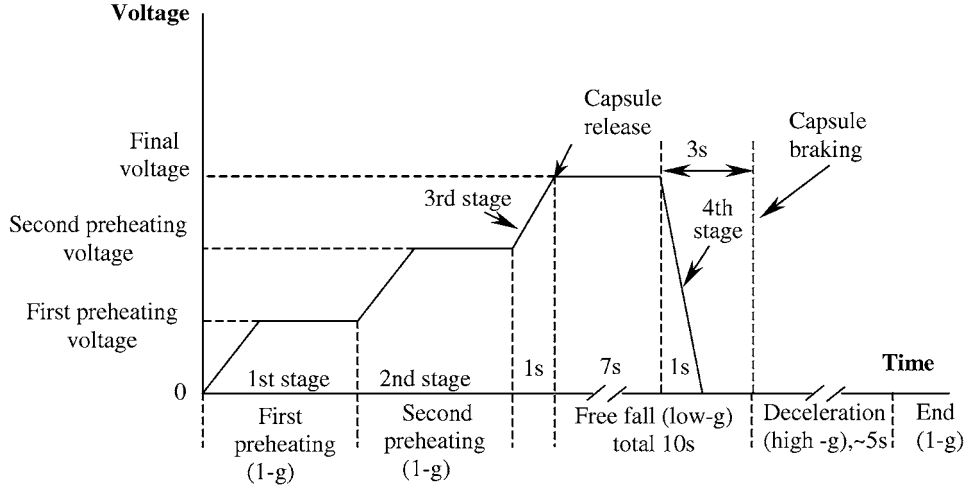

Figure 3 Schematic of a typical heating (voltage-time) schedule for low-gravity experiments at JAMIC.

TABLE I Experimental parameters and shape of the smoke cloud (surrounding the melt) for low gravity experiments at JAMIC

Experiment ID	Weight of sample (mg(±1 mg)	Max. Voltage (Volts)	Max. current (A)	Max. temperature (°C)	Shape of the cloud
NT_8-1Gl	257	Experiment failed due to a problem in the program			
NT_8-2Gl	257	4.6	4.6	765	Spherical
NT_8-3Cu	281	5.45	4.69	830	Spherical
NT_8-4Gl[a]	230	6.55	6.83	(∼1100)	Spherical
NT_8-5Al	150	3.8	6.7	948	Spherical
NT_4-1Cu	150	4.75	7.68	1078	Irregular
NT_4-2Pt	150	4.85	7.1	1083	Irregular
NT_4-3Gl	40	10.15	6.74	(∼1000)	Spherical
NT_4-4Au	150	4.55	7.12	1013	Irregular
NT_4-5Al	150	4.45	6.57	945	Irregular

Note: The maximum temperatures in parenthesis are estimates from similar ground experiments, since no thermocouple was used in these experiments.
[a]Heating coil broke at 4.2 s after capsule release for this experiment.

$<20 \times 10^{-4}$ g ($\pm 5 \times 10^{-4}$ g) during the 10 s of low gravity and reached ∼9 g during capsule deceleration.

Table I summarizes the sample weight, shape of the smoke cloud surrounding the melt and other experimental parameters for the low-g experiments at JAMIC. The experiment is identified by several letters and numbers. The letters and numbers, NT_8 or NT_4, indicate the type of glass. The number after the hyphen denotes the experiment number, and the letters following the number denotes the type of substrate material. For example, the experiment ID "NT_4-5Al" means that this experiment used an NT_4 glass, an alumina substrate and this was the 5th experiment where an NT_4 glass had been used. The substrate materials glass, alumina, copper, gold and platinum used in the present experiments are abbreviated as Gl, Al, Cu, Au, and Pt, respectively.

Although the voltage to the heating coil was programmed to reach its maximum value in 1 s (3rd stage, Fig. 3), the actual voltage did not increase that rapidly. The actual voltage, and hence, the current increased gradually, reaching a maximum at about 6 to 7 s after capsule release as illustrated in Fig. 5 as an example for the NT_8 melt. For some unknown reason, perhaps a defect in the platinum coil, the heating coil voltage for experiment NT_8-4Gl increased abruptly, causing the coil to fail 4.2 s after capsule release. The measured temperature profiles (as a function of low gravity time) for the experiments with NT_8 and NT_4 melts are shown in Fig. 6a and 6b, respectively. No thermocouple was used in experiments NT_8-4Gl and NT_4-3Gl, so the temperatures for these experiments were not measured. The temperatures given in parenthesis in Table I for these experiments have been estimated from similar experiments at 1-g.

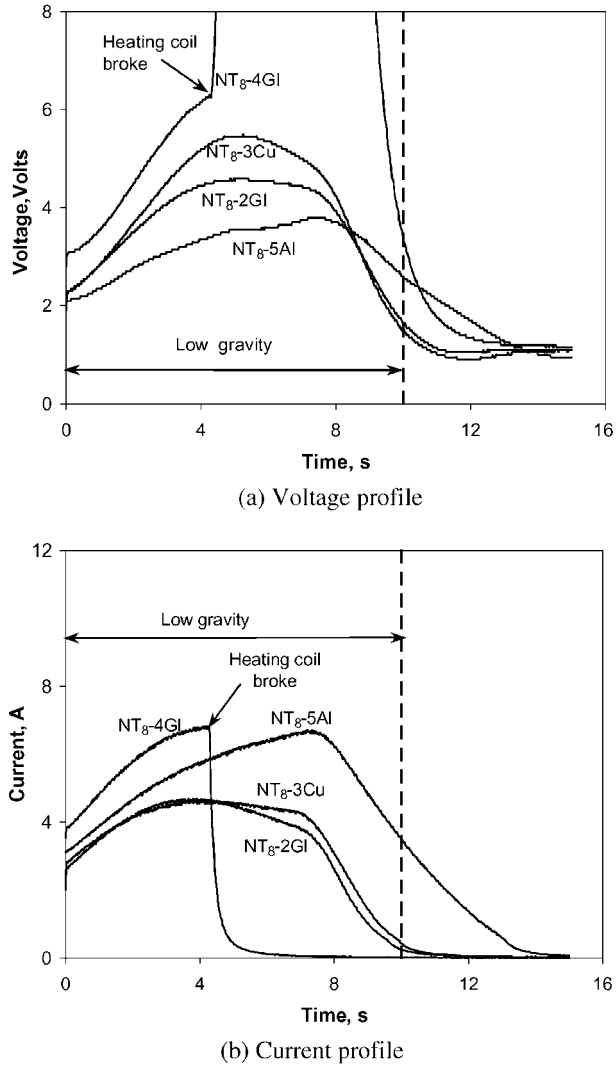

Figure 5 Measured (a) voltage and (b) current to the heating coil in the low gravity experiments at JAMIC with NT_8 melts as a function of time after capsule release.

3.2. Shape of the smoke cloud

The evaporated species from the both NT_8 and NT_4 melts generally formed a spherical cloud of smoke surrounding the melt in low gravity, which broke during capsule deceleration (High-g). The smoke particles were deposited on the inner walls of the glass box (Fig. 1), mostly on the bottom plate. A spherical shape of the cloud in low gravity, an example of which is shown in the 35 mm pictures in Fig. 7a for an NT_8 melt, is expected, since the gravity-driven convection is ideally absent in low gravity, and the cloud should have remained nearly stagnant surrounding the melt. Such a spherical smoke cloud was also observed in our previous [13, 14] low gravity experiments at JAMIC with a NT_4 melt. As shown in Fig. 7a, the size of the cloud increases with increasing time in low gravity. As discussed later, the maximum size of the cloud also depended strongly on the melt temperature and increased with increasing temperature of the melt.

The shape of the cloud depended on several other factors such as the uniformity of heating, amount of

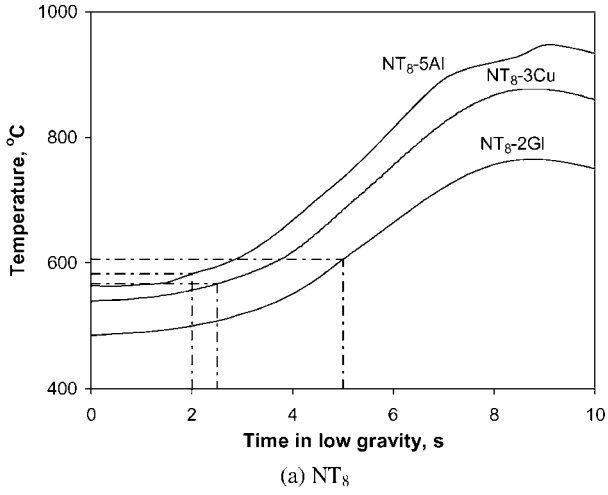

(a) NT_8

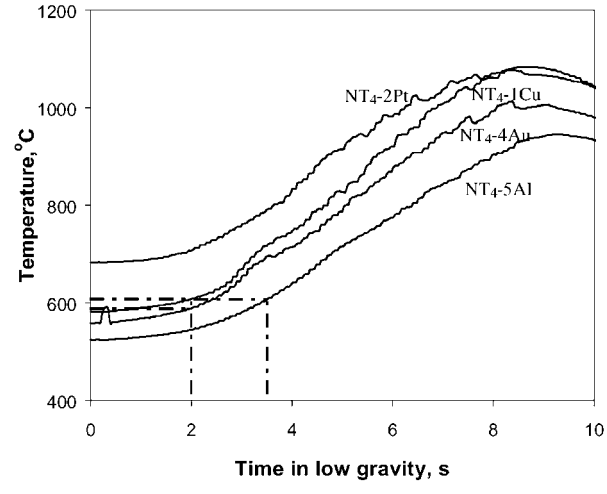

(b) NT_4

Figure 6 Temperature of (a) NT_8 and (b) NT_4 melts in the low gravity experiments at JAMIC as a function of time in low gravity. The broken lines indicate the temperature and time when the cloud surrounding the melt was just visible.

melt, and the presence of entrapped gas bubbles in the melt. Fig. 7b shows a cloud pattern for an NT_8 melt, where the heating was uneven and concentrated at one end of the coil. The video picture for this experiment clearly shows that the heating coil was deformed and was much hotter at one end of the coil. Fig. 7c, which shows the smoke cloud for an NT_4 melt, is a typical example of a cloud when bubbles are present in the glass. The bubbles that were entrapped in the NT_4 glass when it was initially fused to the platinum coil started bursting randomly in low gravity when the melt temperature increased and the melt became fluid. The gas released from these bursting bubbles distorted the vapor cloud in a random way. To obtain a nearly perfect spherical cloud surrounding the melt in low gravity, the heating coil should contain a thin layer of bubble-free glass.

3.3. Size of the smoke cloud

The diameter of the cloud formed in low gravity was measured along the "horizontal" (perpendicular to gravity) and "vertical" (parallel to gravity) directions on the 35 mm pictures (for example, Fig. 7a). The average values of these diameters are plotted in Fig. 8 as a function of low gravity time for different experiments. The cloud grew at a faster rate for the first two seconds, and then grew more slowly with increasing time in low gravity. The maximum diameter of the cloud observed in different experiments ranged between 20 and 25 mm.

For the experiment NT_8-3Cu, the cloud pattern was heavily distorted (Fig. 7b), and a large downward flow of the smoke particles slowed its growth in the horizontal direction. Had the cloud pattern not been distorted (from a typical spherical shape), the expected increase of the cloud diameter with low gravity time for this experiment (NT_8-3Cu) is shown by the dashed line in Fig. 8 on the curve for open triangles. Likewise, the cloud for experiment NT_8-4Gl grew only until the heating coil broke at 4.2 s. The extended dotted line for this curve (open circles) in Fig. 8 shows the expected increase in cloud diameter, assuming the coil would not have broken. All the curves in Fig. 8 are nearly parallel to each other, which suggests that the rate of growth for the size of the cloud with time in low gravity was nearly the same for all the four experiments.

The cloud became visible only when its diameter exceeded about 10 mm, see the horizontal band in Fig. 8. The time (in low gravity) when the cloud just became visible was determined from Fig. 8, and used in Fig. 6a to determine whether the melt temperature has any effect on the minimum detectable size of the cloud, see the dashed lines in Fig. 6a for the NT_8 melts. Similar analysis was also performed for the just detectable size of the cloud from the NT_4 melts, see Fig. 6b. As shown in Fig. 6, the vapor cloud just became visible when the melt temperature was $585 \pm 25°C$ for both NT_8 and NT_4 melts. It is to be noted that both NT_8 and NT_4 glasses melt at about 470°C.

It appears that the temperature within a spherical region of 10 mm diameter surrounding the melt was so high that the evaporating species in this region remained in the gaseous (vapor) phase, and there was no condensation of the evaporating species in this region. Although the diameter of this "gaseous" region is expected to be larger for melts at higher temperature, any temperature dependence of the diameter in this region could not be detected for the temperatures used in these experiments.

The melt temperatures determined from Fig. 6a at the 6th second in low gravity for the NT_8 melts are shown on each curve in Fig. 8, see the temperatures shown on the vertical dashed line. These results show that the diameter of the cloud is larger at any given time as the melt temperature increases. To understand more about the dependence of cloud size on melt temperature, the time values in Fig. 8 (horizontal axis) were replaced by their corresponding temperatures (determined from Fig. 6a) to obtain a cloud diameter vs temperature plot as shown in Fig. 9. Clearly, the size of the vapor cloud increases with increasing melt temperature in nearly the same fashion for all the experiments with NT_8 melts. The double-headed horizontal arrow in Fig. 9 shows the temperature range ($585 \pm 25°C$) when the cloud became just visible.

For the NT_4 melt, a nearly perfect spherical cloud was obtained in low gravity only in experiment NT_4-3Gl, see Table I. The smoke from the other experiments did

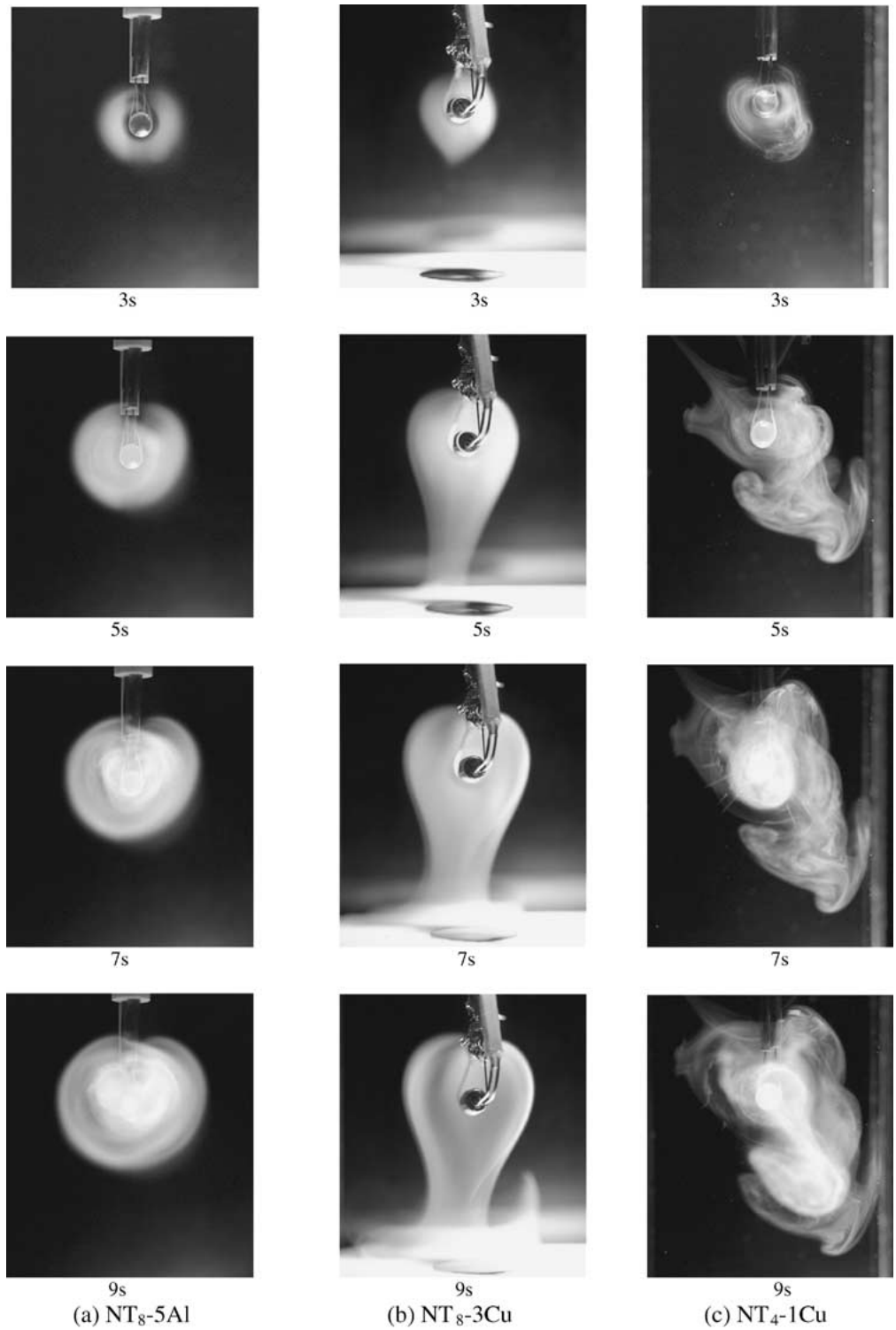

Figure 7 35 mm pictures of the cloud formed at different low gravity time by the evaporating species from low gravity experiments at JAMIC, (a) NT_8-5Al, (b) NT_8-3Cu and (c) NT_4-1Cu.

not form a spherical cloud because of gas bubbles in the melt, which burst in low gravity. The gas released by the bursting bubbles distorted the usual spherical shape of the cloud, thereby, making the shape highly irregular such as the one shown in Fig. 7c. This irregular shape made it difficult to measure the growth of the cloud as a function of low gravity time or melt temperature.

The diameter of the smoke cloud for experiment NT_4-3Gl, whose cloud had a nearly spherical shape throughout the low gravity period, was measured from the 35 mm pictures and is plotted in Fig. 10 as a function of low gravity time. Fig. 10 also includes, for comparison, similar data from our previous experiments [13] conducted by evaporating a similar NT_4 melt in the JAMIC drop shaft in 1993. The diameter of the cloud for the present experiment NT_4-3Gl is smaller than that for the cloud from our previous drop experiment at JAMIC [13] at all times. The smaller size for the cloud in the present experiment suggests that the melt temperature was slightly less than the melt temperature in the previous experiment.

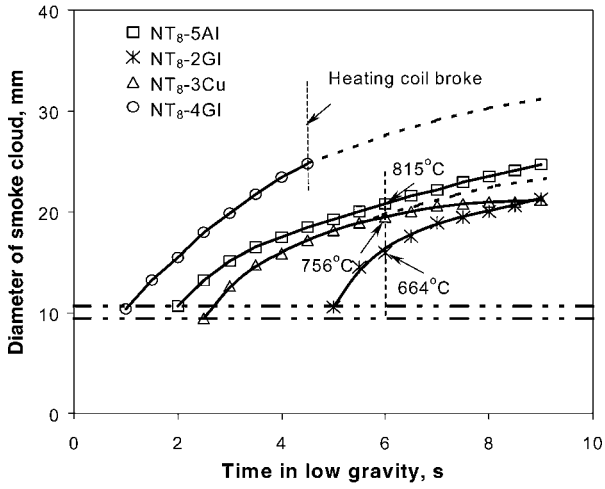

Figure 8 Diameter of the cloud as a function of time in low gravity from evaporation of NT_8 melts. The horizontal band made by two broken lines indicates the range in minimum diameter when the vapor cloud was just visible. The temperatures shown on a vertical dashed line are the temperatures of melts for different experiments (from Fig. 6a) at the 6th second after capsule release.

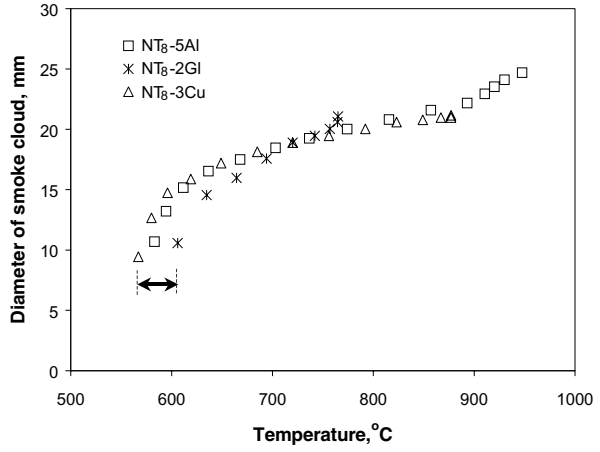

Figure 9 Diameter of the cloud from evaporation of NT_8 melts in low gravity (JAMIC) as a function of melt temperature (reconstructed from the curves in Figs 6a and 8).

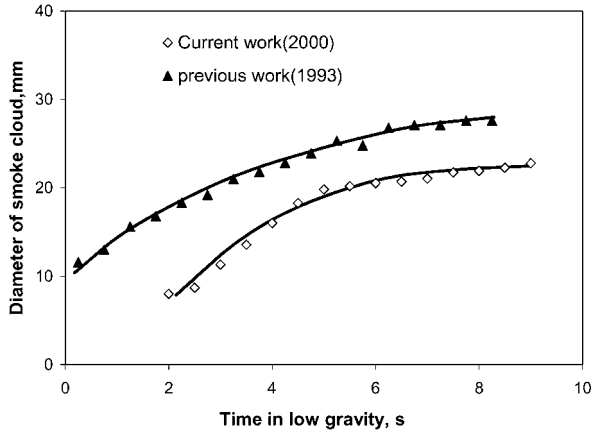

Figure 10 Diameter of the cloud formed from evaporation of NT_4 melts as a function of time in low gravity experiments at JAMIC.

3.4. Microspheres formed from vapor

As mentioned earlier, the cloud of smoke formed surrounding the melt in low gravity, broke during high-g deceleration of the capsule and the smoke particles deposited mostly on the bottom plate of the glass box (Fig. 1). When analyzed by scanning electron microscopy (SEM) and energy dispersive x-ray analysis (EDS), the substance deposited on the bottom plate consisted of small spherical particles (microspheres) of pure TeO_2. No sodium was detected. Representative SEM pictures for the TeO_2 microsphere formed from the vapor of NT_8 and NT_4 melts are shown in Fig. 11. TeO_2 microspheres condensed from vapor was also observed in our previous drop experiments with NT_4 glass [13, 14]. These microspheres were found to be amorphous by XRD.

Results from the present and previous [13, 14] experiments demonstrate that evaporation of sodium-tellurite melts, regardless of composition, results in the formation of TeO_2 spheres. The vapor pressure of TeO_2($\sim 1.3 \times 10^{-1}$ mm Hg) at $\sim$730°C is about two orders of magnitude higher than that of Na_2O ($\sim 1.5 \times 10^{-3}$ mm Hg),[15] so, it is likely that TeO_2 will evaporate more profusely than Na_2O from these sodium-tellurite melts. However, our ground-based work suggests that it is not TeO_2, but either tellurium ions or elemental tellurium evaporate from the melt, and then react with oxygen in the surrounding air to form TeO_2. This conclusion was reached after comparing the Auger spectra for the material produced by evaporating an NT_8 melt in an inert (argon) atmosphere with that for the material produced by evaporating the same melt in air. While the material produced in the argon atmosphere consisted mostly of elemental Te and very little oxygen (<10 atom%), the material produced in air contained both Te and oxygen. The atom percent of Te and O calculated from the Auger spectrum for the material produced in air was in the proportion corresponding to TeO_2. The small amount of oxygen present in the Auger spectrum for the material produced in argon may be due to impurities (oxygen) present in the argon, or more likely, to a leak in the box in which the experiment was conducted, which permitted a small amount of oxygen to enter.

The diameter of the TeO_2 microspheres as measured by SEM is given in Table II for different low gravity experiments along with the diameter of TeO_2 microspheres prepared from similar experiments at 1-g.

Also included in Table II are the diameter of the TeO_2 microspheres from our previous [13] low gravity experiments with the NT_4 melts, the maximum melt temperature (column 2), and the duration for which the smoke cloud surrounding the melt existed in low gravity (column 5). The results in Table II generally show that (1) the average size of the TeO_2 microspheres from either low gravity or 1-g experiments is the same for the NT_8 and NT_4 melts, i.e., the size of the microspheres is independent of melt composition, (2) the size of the microspheres from low gravity experiments is 5 to 10 times larger than similar microspheres prepared at 1-g, (3) for comparable low gravity duration, the size of the microspheres increased with increasing melt temperature, and (4) for comparable melt temperature, the size of the microspheres increased with increasing time in low gravity. The size of the TeO_2 microspheres from the present and previous [13] low gravity experiments is also comparable.

TABLE II Size range of TeO_2 microspheres from different low gravity (JAMIC) and ground experiments

Experiment ID	Max. melt temperature (°C)	Range of diameter of TeO_2 spheres (μm)	Diameter of majority (60–70%) spheres (μm)	Duration of smoke cloud in low-g[b] (s)
NT_8-2Gl	765	0.05–0.5	0.1–0.3	4
NT_8-3Cu	830	0.1– 2	0.5–1	7
NT_8-4Gl[a]	(∼1100)	0.05–10	0.5–2	3.5
NT_8-5Al	948	0.1–20	1–5	7
Ground(NT_8-Gl)	900–1000	0.05–0.5	0.1–0.2	–
NT_4-1Cu	1078	0.02–20	1–5	7
NT_4-2Pt	1083	0.05–20	1–5	8
NT_4-3Gl	(∼1000)	0.05–5	0.5–1	7.5
NT_4-4Au	1013	0.03–15	1–5	7.5
NT_4-5Al	945	0.02–5	0.1–0.5	6
Ground(NT_4-Gl)	900–1000	0.05–0.5	0.1–0.2	–
Previous Expt. (NT_4-Gl)[13]	(>1200)	0.5–8	3–5	8

Note: The maximum temperatures in parenthesis are estimates from similar ground experiments, since no thermocouple was used in these experiments.
[a]Heating coil broke at 4.2 s after capsule release for this experiment.
[b]This duration is from the time a cloud just became visible to the time the capsule started decelerating.

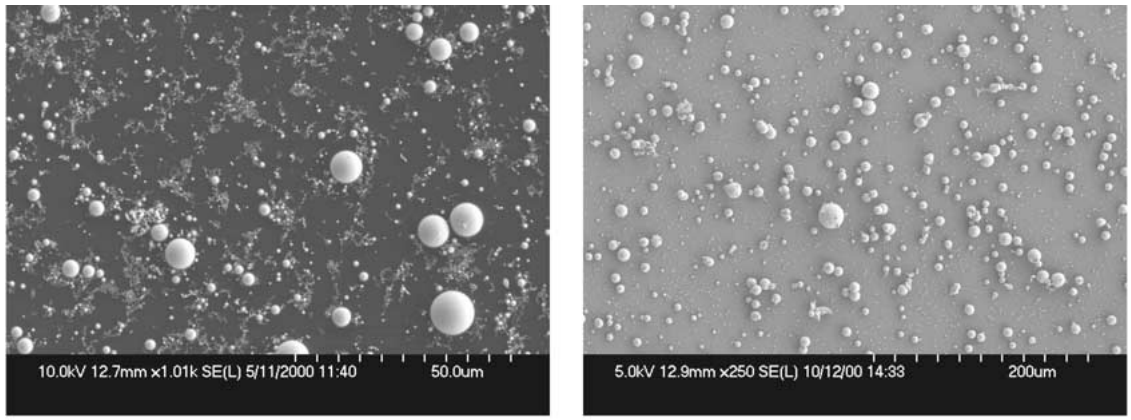

(a) NT_8-4Gl (b) NT_4-2Pt

Figure 11 SEM of TeO_2 microspheres deposited on the bottom plate in low gravity (JAMIC) experiments with NT_8 and NT_4 melts.

A conceptual scenario for forming solid TeO_2 spheres from vapor is shown schematically in Fig. 12. Close to the heating coil, out to a distance of about 5 mm from the center of the coil (region I), the temperature is high enough that the evaporating species is present as a gas (vapor), and therefore, not visible.

In region II, which is farther from the heating coil (>5 mm from the center of the coil), the temperature is low enough for the TeO_2 to condense to form liquid TeO_2 droplets, which form an optically translucent (visible) cloud. The perfect spherical shape of the TeO_2 microspheres indicates that they existed in the liquid state (droplet). With time these droplets grow in size by additional condensation on them and/or by coalescing with other droplets. These liquid droplets tend to solidify as they move further away from the heating coil, region III, where the temperature is lower than in region II.

A higher temperature of the heating coil increases the rate of evaporation i.e., evaporates more gaseous material. This increases the probability for both the processes, namely, additional condensation and coalescence of two or more droplets while they are in the liquid state, which can account for a larger average size of the TeO_2 spheres for higher temperature melts.

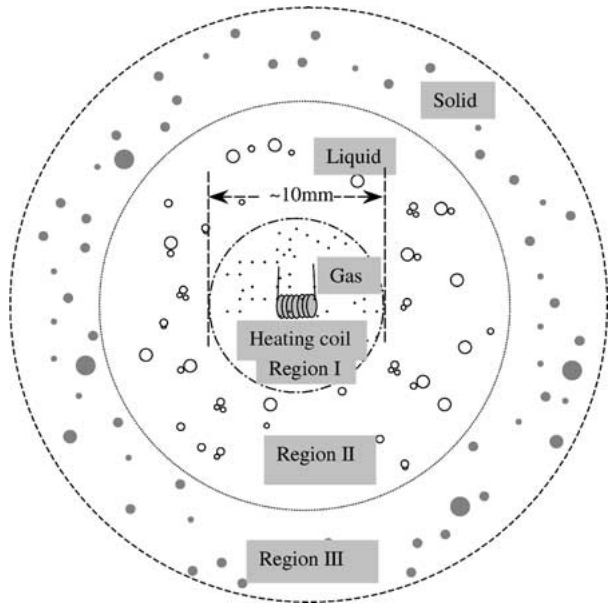

Figure 12 Schematic for forming solid TeO_2 microspheres from the vapor of Na_2O-TeO_2 melts in low gravity. Region I (temp.>760°C) contains gaseous species (Te atoms or ions) which react with oxygen to form TeO_2. Region II (lower temperature ∼470 to 760°C) contains molten droplets of TeO_2 that grow by condensation or coalescence. Region III (temperature <470°C) contains solid TeO_2 microspheres.

Unlike the clouds in low gravity, the evaporating species from similar melts at 1-g do not form a stagnant cloud around a hot melt, but rapidly move upwards, due to gravity-driven convection. These droplets are quickly transported to colder region where these tiny droplets do not have sufficient time to grow. As a result, the size of TeO_2 microspheres prepared at 1-g is much smaller (5 to 10 times) than that of the TeO_2 microspheres prepared in low gravity, see Table II.

4. Conclusion

The species evaporated from a sodium tellurite melt in low gravity generally formed a spherical cloud of smoke surrounding the melt. The shape of the cloud was also influenced by the uniformity of heating, amount of melt and the presence of any gas bubbles in the melt which could burst and deform the cloud. The vapor from these melts produced perfectly spherical particles (microspheres) of vitreous TeO_2, ranging in size from 0.05 to 20 μm in diameter. The diameter of the TeO_2 microspheres increased with increasing melt temperature or with increasing time the cloud existed in low gravity and was 5 to 10 times larger than those prepared from similar experiments at 1-g. It is expected that the size of TeO_2 microspheres can be increased considerably if similar evaporation experiments are conducted for longer time periods in microgravity such as in space shuttle or space station.

Acknowledgment

The work was partly supported by National Aeronautics and Space Administration (NASA), contract # NAG8-1465. The authors also greatly appreciate the help and cooperation, of the following persons and organizations: Dr. Hajimu Wakabayashi of Nihon Yamamura Glass Co. (Japan), Dr. Hisao Azuma of Osaka Prefecture University (Japan), Japan Microgravity Center (JAMIC), Japan, and New Energy & Industrial Technology Development Organization (NEDO), Japan.

References

1. C. BARTA, L. STOURAC, A. TRISKA, J. KOCKA and M. ZAVETOVA, *J. Non-Cryst. Solids* **35/36** (1980) 1239.
2. C. BARTA, J. TRNKA, A. TRISKA and M. FRUMAR, *Adv.Space Res.* **1**(5) (1981) 121.
3. G. T. PETROVSKII, V. V. RYUMIN and I. V. SEMESHKIN, *Steklo i Keramika* **1** (1983) 5.
4. G. H. FRISCHAT, *J. Non-Cryst. Solids* **183** (1995) 92.
5. C. S. RAY and D. E. DAY, *Mat. Res. Soc. Symp. Proc.* **87** (1987) 239.
6. D. S. TUCKER, G. L. WORKMAN and G. A. SMITH, *J. Mater.Res.* **12**(9) (1997) 2223.
7. D. S. TUCKER, R. N. SCRIPA, B. WANG and J. M. RIGSBEE, Proc. 18th Int. Cong. On Glass, July 1998, San Francisco (available in CD Rom).
8. J. A. NUTH and B. DONN, *J. Chem. Phys.* **77** (1982) 2639.
9. D. E. DAY and G. H. EHRHARDT, U.S. Patent no. 5,001,677; 30 April 1991.
10. J. E. WHITE and D. E. DAY, *Key Engineering Materials* **94/95** (1994) 181.
11. S. S. SOSA, *Materials Research Society (MRS) Bulletin* (February 2001) 88.
12. M. C. LEE, J. M. KENDALL, D. D. ELLEMAN, W.-K. RHIM, R. S. HELIZON, C. L. YONGBERG, I.-A. FENG and T. G. WANG, *Mat. Res. Soc. Symp. Proc.* **9** (1982) 95.
13. C. S. RAY, D. E. DAY, M. MAKIHARA and J. HAYAKAWA, in Proceedings of 19th ISTS. Hakushinsha Co., Tokyo, Japan, 1994, edited by M. Hinada, p. 651.
14. M. MAKIHARA, C. S. RAY and D. E. DAY, *Proce. SPIE* **3792** (1999) 209.
15. N. KITAMURA, M. MAKIHARA, T. SATO, M. HAMAI, I. MOGE, S. AWAJI, K. WATANABE and M. MOTOKAWA, *JASMA* **17** (JASMAC-16 Abstract) (2000) 102.

Received 19 September 2001
and accepted 27 March 2002